멤브레인(Membrane Journal)
Vol. 25 No. 3 June, 2015, 268-275

Print ISSN: 1226-0088
Online ISSN: 2288-7253
DOI: http://dx.doi.org/10.14579/MEMBRANE_JOURNAL.2015.25.3.268

정수처리를 위한 응집-침지식 정밀여과 모듈의 유체유속 및 국부오염

최 영 근 · 김 현 철* · 노 수 홍**,†

주흥환경(주) 기술연구소, *세종대학교 물자원연구소, **연세대학교 환경공학부
(2015년 5월 21일 접수, 2015년 6월 15일 수정, 2015년 6월 19일 채택)

Liquid Velocity and Local Fouling in Coagulation-submerged Microfiltration Module for Drinking Water Treatment

Youngkeun Choi, Hyun-Chul Kim*, and Soohong Noh,†**

Juheung Entech Co., Ltd, Yongin 448-160
*Water Resources Research Institute, Sejong University, Seoul 143-747, Korea
**Department of Environmental Engineering, Yonsei University, Wonju 220-710, Korea
(Received May 21, 2015, Revised June 15, 2015, Accepted June 19, 2015)

요 약: 침지식 분리막 모듈에서 공기강도에 따른 분리막 위치에 대한 오염을 조사하였다. 분리막의 충진밀도가 낮은 곳에서 높은 유체 유속을 나타내었으며, 유체 속도는 기-액 주입률에 비례하였다. 전단응력은 기-액 주입률 및 유체 유속에 비례하였다. 비가역오염(R_{ir})은 흡입 압력이 가까운 부분에서 가장 높게 나타났다(position 1). 비가역오염에 대한 저항과 분리막 고유 저항의 비(R_{ir}/R_m) 및 비가역오염에 대한 저항과 가역오염의 저항의 비(R_{ir}/R_r)도 position 1에서 가장 높게 조사되었다. 비가역오염(R_{ir})은 흡입 압력이 높은 곳인 position 1에 오염물질이 축적되어진 결과이다. 분리막 위치에 따른 오염현상은 모듈 디자인 최적화에 중요한 인자임을 알았다.

Abstract: Effects of aeration intensity on local fouling were investigated in submerged membrane modules. Higher liquid velocities were observed at the section with the lower fiber packing density. The liquid velocity is increased with increasing the gas-liquid injection factor. The high shear stress coincided with the high liquid velocity. The shear stress increases with the increasing of gas-liquid injection factor and the liquid velocity improves with the increasing of gas-liquid injection factor. Irreversible fouling resistance (R_{ir}) of the fiber position is significant in a local region of high suction pressure near the suction point of the fiber (position 1). The ratio of R_{ir}/R_m and R_{ir}/R_r of position 1 was highest compared to the position 2 and 3. Irreversible fouling resistances results confirmed the preferential deposition of foulants near the suction part of the fiber where the local suction pressure is the highest and correspondingly, more particles are accumulated to the membrane surface. The effects of local fouling along the fiber length are significant factors to optimize the design of submerged modules.

***Keywords**: Aeration intensity, Liquid velocity, Local fouling, Submerged membrane module, irreversible fouling*

1. Introduction

Air is injected at the bottom of a submerged membrane in order to reduce fouling of the membrane surface or clogging of the pore. Air is often introduced below the membrane assembly and is supposed to be ideally distributed to optimise the air scouring action across the membrane surface. The optimum air flow and flow pattern for this purpose are subject to each module configuration. Membrane aeration contributes

†Corresponding author(e-mail: drnoh@yonsei.ac.kr, http://orcid.org/0000-0001-8446-2840)

significantly to the overall energy demand. The design and optimisation of the aeration requires knowledge on the effective distribution of air in the whole membrane module, which impacts on the membrane fouling reduction. Improving hydrodynamics within the membrane cassette could reduce the aeration requirement and reduce the membrane fouling.

Recently some studies have shown of gas-liquid flow techniques in concentrated solutions during ultrafiltration (UF) in order to investigate the fouling mechanisms for different applications and for different membrane geometries (hollow fiber[1], flat sheet[2], tubular[3] and freely end hollow fiber[4]). Application of gas-liquid flow for microfiltration (MF) is based on change of hydrodynamic conditions inside the MF module which positively increase the wall shear stress, preventing the membrane fouling and enhancing the mass transfer of separated compound (hollow fiber[5,6], tubular[7], flat sheet[8-10]. Vertical or horizontal types are generally used in the large applications. Horizontal type configuration showed good fouling reduction[2].

Alleviating membrane fouling in the submerged membrane is still an area of intense research interests. The local fouling could be strongly dependent upon characteristics of foulant materials and membrane module configuration. The extent of the reduction in membrane fouling produced by aeration may depend upon fiber configuration although relatively little has been reported in the literature. Particles accumulate faster in a local region of high flux near the suction-end of the fiber where the transmembrane pressure (TMP) is highest along the fiber. Morphological examinations have confirmed the preferential deposition of particles near the suction-end of the fiber where the local flux is the highest[11]. The importance of fiber length in submerged hollow module was investigated with the hydraulic model[12]. This model shows that the local flux gradually increases along the fiber length such that the flux is higher than length-averaged value near the open end of the fiber. According to this model, the extent to which flux varies along the fiber increases with lower membrane resistance. At start up of filtration, the TMP near the open end of the fiber exceeds the length-averaged TMP and thus, particle deposition can occur in this region whereas further down the fiber the local TMP is lower and foulants do not deposit[13]. The result is a shift in location of particle deposition with aeration efficiency. Deposition distribution, in other words, fouling location should be determinants of back transport velocity and the effectiveness of liquid velocity caused by aeration. Since the local fouling can determine the overall performance in submerged membrane system.

The objective of this study was to characterize the flow distribution inside a commercial submerged hollow fiber MF module. In previous studies, we have measured superficial liquid velocity on the top of the MF and UF membrane module[14]. The present study shows how local measurements can help to improve understanding of the two-phase hydrodynamics in a submerged hollow fiber MF module. Furthermore, effects of the chemical cleaning on local fouling were also investigated.

2. Materials and Method

2.1. Liquid velocity

The experimental setup consists of a MF reactor tank with the dimension z = 3 m, y = 1.79 m and x = 1.79 m. The tank is equipped with Cleanfil-S10 (Kolon, South Korea) cassette made of 30 MF elements. Each element consists of a bundle of hollow fiber membranes and the total membrane surface area of the cassette is equal to 600 m^2. Sparging air flow along the membrane surface is created by coarse bubble aeration at the bottom of the membranes (Fig. 1). The air is introduced through three perforated pipes with holes of 5 mm of diameter connected to a blower which allows an air flow rate up to 120 Nm^3/hr. The distance between the reactor wall and the module is approximately 13.5 cm. The so-called airlift reactor is divided into two vertical zones connected at the top and the bottom. The experimental setup used to measure the liquid velocity is shown in Fig. 1 (a). For this

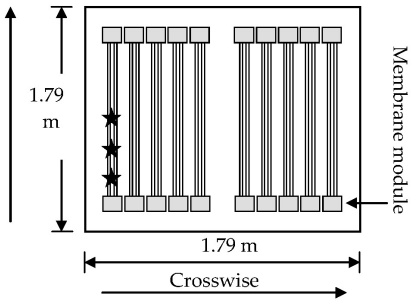

(a) Horizontal section

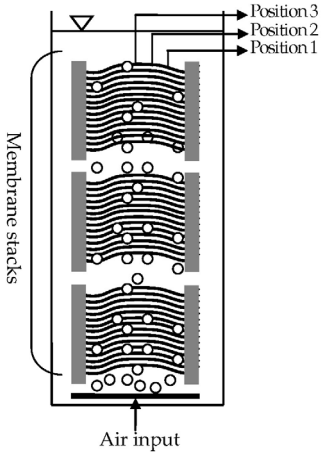

(b) Cross section

Fig. 1. Schematic diagram for MF plant (★ indicates velocity measuring and fibers sampling positions).

test, an open channel flow meter (BFM002, Valeport), signal transmitter and personal computer for the data acquisition were used. The flow meter was tightly held in order to stabilize the measuring impeller of flow meter. Liquid velocity measurements were performed along the top side of the modules (Fig. 1 (a)) for MF reactor tank. The gas flow rates were varied between 60 to 130 Nm^3/hr, which corresponds to an aeration intensity 0.1 to 0.22 m/s with MF reactor tank.

This study was run with tap water and air without filtration because the main objective was to characterize the flow induced by the aeration. The two phase flow pattern depends on the air-injection factor (ε) defined as[15] :

$$\varepsilon = \frac{U_{gs}}{U_{gs} + U_{ls}} \quad (1)$$

Table 1. Configuration and Experimental Conditions of the Membrane Plant

Items	MF module
Material	PVDF
Configuration	Horizontal type
Area (m^2)	600
Air flow rate (m^3/hr)	60 - 130
*Aeration intensity (m/hr)	0.1 - 0.22

*Air flow (m^3/min)/membrane area (m^2)

$$U_{gs} = \frac{U_g}{S} \quad (2)$$

$$U_{ls} = \frac{U_l}{S} \quad (3)$$

where, U_{gs} and U_{ls} are the superficial gas and liquid velocity (m/sec), respectively. U_g and U_l are the gas and liquid flow rate, respectively, and S is the cross section area (m^2) with microfiltration plant. The flow pattern, as classified according to the value of ε is defined as[15] :

- bubble flow, $\varepsilon < 0.2$
- slug flow, $0.2 < \varepsilon < 0.9$
- annular flow, $0.9 > \varepsilon$

The dimensional parameters for the MF membrane module cassette used in this study are shown in Table 1.

2.2. Resistance investigations with chemical cleaning

Membrane resistances were estimated to investigate membrane fouling at the end of operation (after six month) of the coagulant-submerged membrane system. The membrane samples at the same positions were also taken from upper membrane stack (shown in Fig. 1). The fiber samples were taken along the fiber length every 0.5 m from the open end of the fiber, which was designated as positions 1 (0.1 m), 2 (0.3 m) and 3 (0.5 m). Membrane permeability after chemical cleaning for each segment of hollow fiber membrane was

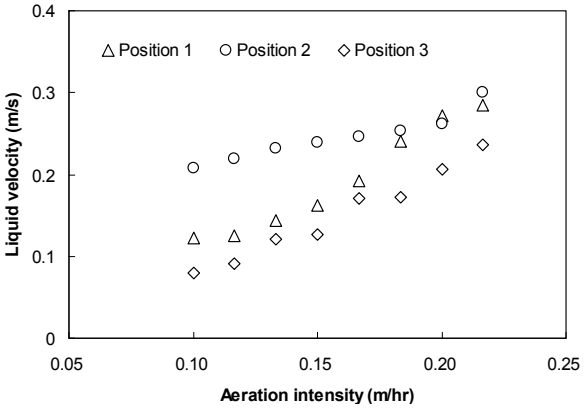

Fig. 2. The liquid velocity on aeration intensity along the fiber positions.

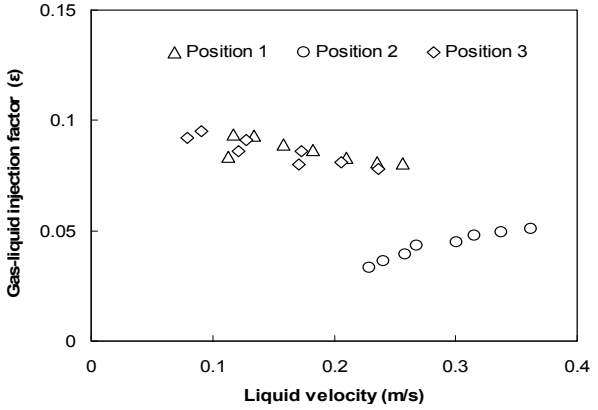

Fig. 3. Gas-liquid injection factor on liquid velocity along the fiber positions.

measured to determine irreversible fouling resistance by using resistance-in-series model.

$$J = \frac{TMP}{\mu R_t} = \frac{TMP}{\mu(R_m + R_r + R_{ir})} \quad (4)$$

Where, J is the permeate water flux (LMH), TMP is the transmembrane pressure (Pa), μ is the water viscosity (Pa · s). R_t is the total filtration resistance (m^{-1}), R_m is the intrinsic membrane filtration resistance (m^{-1}), R_r is the chemically reversible resistance (m^{-1}), and R_{ir} is the chemically irreversible filtration resistance (m^{-1}). Reversible filtration resistance, denoted in this paper by R_r can only be eliminated by use of chemical reagents.

3. Results and Discussion

3.1. Liquid velocity and gas-liquid injection factor at different positions

The liquid velocity and gas-liquid injection factor are presented in Fig. 2 and 3 for the three positions. When comparing the evolution of liquid velocity with aeration intensity in Fig. 2 and evolution of gas-liquid injection factor with liquid velocity in Fig. 3. The increase of aeration intensity implies a larger liquid movement. When increasing the aeration intensity from 0.1 to 0.22 m/hr, the liquid velocity increase from 0.12 to 0.28 m/s at position 1, from 0.21 to 0.3 m/s at position 2 and from 0.08 to 0.24 m/s at position 3, respectively. This liquid velocity is however, not uniform at the vertically positions. Between position 1 and 3, there is sharp increase of liquid velocity with aeration intensity. But, position 2 shows slow increase of liquid velocity with aeration intensity. However, the liquid velocity of position 2 is higher than position 1 and 3. The lower liquid velocity in position 1 and 3 can be explained by the fact that the path of the gas was not rectilinear. Therefore, the liquid velocities by aeration have not only vertical motion but also a lateral motion and they may flow towards the central zone. At point of air injection in Fig. 1 (b), from position 3 to 1, there is long length of the air injection point (Fig. 1 (b)). Position 3 is the entrance part of aeration pipe and position 1 is the rear part of aeration pipe. Position 3 may create a recirculation in the liquid above the rear part zone (position 2 and 1), leading to a lateral motion of the gas bubbles. This phenomenon has been described by various authors[16-18]. In other words, the kinetic energy at the input is much higher than the frictional pressure drop along the aeration pipe, the holes at the rear discharge more than the entrance holes. The liquid velocity of position 1 is similar to that of position 3 up to 0.18 m/hr of aeration intensity. The dependence of liquid velocity on aera tion intensity has no obstruction object. The fiber packing density of position 1 is higher than position 2 and 3. Consequently, this position leads to the spread and break-up of the gas bubble resulting in a decrease

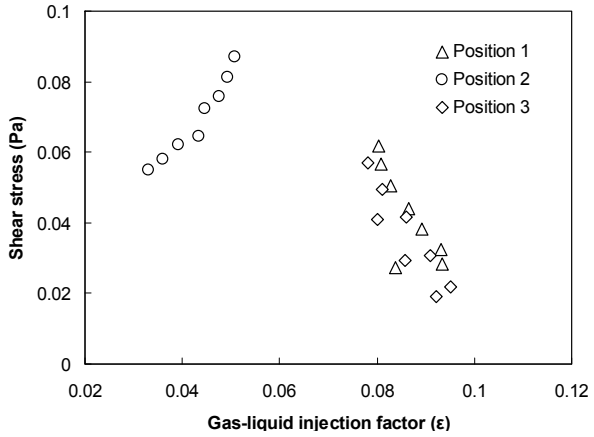

Fig. 4. Shear stress on gas-liquid injection factor along the fiber positions.

of the liquid velocity. However, the liquid velocity of position 1 is similar to that of position 2 from 0.18 m/hr of aeration intensity. At above 0.18 m/hr of aeration intensity, the higher liquid velocity measured at position 1 might be due to the coalescence phenomena[18-20]. In our case, coalescence and break-up are in position 1.

The gas-liquid injection factor is presented in Fig. 3 for the three positions. The distribution of the air is less uniform between position 1 and 3 versus position 2 of the gas-liquid injection factor. The gas-liquid injection factor decreased with increasing the liquid velocity of position 1 and 3. But, the gas-liquid injection factor of position 2 increased with increasing the liquid velocity. The gas-liquid injection factor of position 1 is similar to that of position 3. In the position 2, the gas-liquid injection factor is proportional to the increase due to the production of higher bubbles by increasing of the aeration. Moreover, the gas bubbles were profitable rectilinear, therefore, the liquid velocity is increased with increasing the gas-liquid injection factor[18].

3.2. Links between shear stress and gas-liquid injection factor

The shear stress (τ) is given in Eqs. (5)[21].

$$\tau = \mu \frac{6\nu}{b} \tag{5}$$

Where, τ is the shear stress (Pa), ν is the liquid velocity (m/s), μ is the dynamic viscosity (Pa・s), b is the membrane height (m).

Fig. 4 shows the shear stress distribution on the gas-liquid injection factor at three different positions. The maximum shear stress of position 1 and 3 is almost the same. The maximum shear stress of position 2 is higher than those of position 1 and 3. In this result that the regions of high shear stress coincide with the position where there is high liquid velocity (Fig. 2) with high gas-liquid injection factor (Fig. 3). The regions of high shear stress coincide with the presence of bubble. This phenomenon has been observed experimentally[22-24], where the shear stress was higher in the presence of bubbles. Even though, the superficial liquid velocity was similar in both cases. Thus, position of higher liquid velocity is exposed to a high shear stress. The shear stress increases with the increasing of gas-liquid injection factor and the liquid velocity improves with the increasing of gas-liquid injection factor. The shear stress is higher position where the degree of fouling was very low. As the aeration intensity is increased, the system becomes more unstable. The majority of gas bubbles start to migrate to the top of the membrane module and move vigorously in random manner. There is the strong rising of liquid inside the membrane fibers. There is little migration of gas bubbles towards the different regions. Thus, with higher shear stress, there is a straight liquid and uniform path at the position which helps to alleviate fouling.

3.3. Fractionation of the fouling layer

Coagulation-submerged microfiltration system was applied at 'K' Drinking Water Treatment Plant (Seoul, South Korea). Raw water flow rate in the system ranged from 520-580 m^3/day. The recovery rate was set at 99%. Submerged membrane plant was operated at constant flux mode of 40 LMH. Air flow rate was constant at 120 Nm^3/hr, which corresponds to an aeration intensity 0.2 m/hr. Backwashing using permeate was conducted for 30-s every 15-min of backwashing frequency.

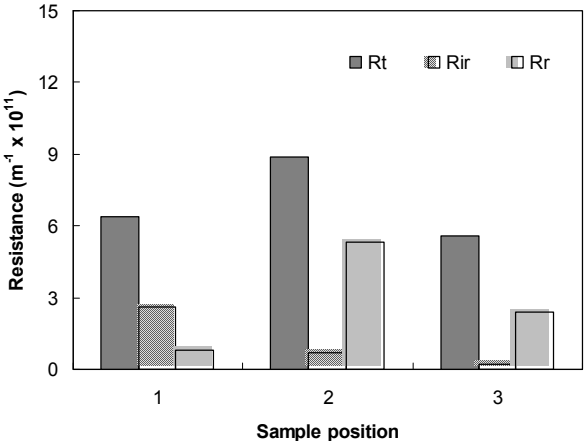

Fig. 5. Hydraulic resistances of the different fractions for the fiber positions.

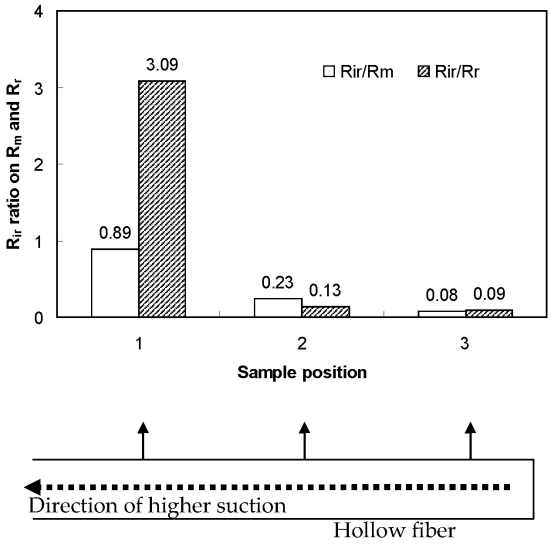

Fig. 6. The ratio of hydraulic resistances on irreversible fouling.

Fig. 5 displays the hydraulic resistances of the different fractions in the different position of the fibers after 6 months of operation and shows the contribution of the different fouling fractions to the total fouling. The position 2 produces the highest total fouling resistances (R_t) and the position 3 the lowest. The higher R_t of position 2 are caused by the reversible cake layers (R_r) attached on the membranes, which can be removed by rinsing the membrane. Consequently, R_r of the position 2 is highest comparing to the other position. Irreversible fouling resistance (R_{ir}) of the fiber position is significant in a local region of high suction pressure near the suction point of the fiber (position 1) than elsewhere along the fiber (position 2 and 3). As the local suction pressure increases, a more compressed fouling layer is formed, resulting in an irreversible fouling layer[25]. Moreover, R_{ir} was found to be big compared to the position 2 and 3, corresponding to the advantage of fiber looseness with low packing density.

The ratio of R_{ir}/R_m and R_{ir}/R_r at the suction part along the fiber position provides a degree of contribution to irreversible fouling resistance of R_{ir}. The ratio of R_{ir}/R_m and R_{ir}/R_r are shown in Fig. 6. The ratio of R_{ir}/R_m and R_{ir}/R_r of position 1 was highest comparing to the position 2 and 3. The ratio between R_{ir}/R_m and R_{ir}/R_r were almost the same. That is, the irreversible foulants accumulate to a far extent by higher suction pressure. At position 2 and 3 of low fiber density, those positions are sufficiently effective in removing foulant. Especially, R_{ir}/R_r value of the position 1 was magnitude higher than other position. This value indicates that the most irreversible fouling layer of the membrane is formed due to internal pore fouling and adsorption on the membrane surface[26].

Liquid velocity induced by aeration tends to reduce the magnitude of readily removable resistance (R_r) and the irreversible resistance (R_{ir})[12]. The reduced fouling resistance must be due to the result of the increased back transport induced by aeration. Liquid velocities among position 1, 2, and 3 follow the order of : 2 > 1 > 3 (Fig. 2). There are not in agreement of R_{ir} and R_r in relation to liquid velocity in Fig. 5. Therefore, control of the reversible and the irreversible fouling resistances is needs both higher liquid velocity and lower packing density. Additionally, lower suction pressure part can be more alleviated in spite of lower liquid velocity at position 3 (Figs. 5, 6).

4. Conclusions

In present study characteristics of liquid velocity and local fouling of pilot-scale submerge membrane modules was studied. The investigation the following con-

clusions can be made :

The liquid velocity behavior of submerged membrane modules depends on the imposed aeration intensity, and the local position. When increasing the aeration intensity from 0.1 to 0.22 m/hr, the liquid velocity increased from 0.12 to 0.28 m/s at position 1, from 0.21 to 0.3 m/s at position 2 and from 0.08 to 0.24 m/s at position 3, respectively. The gas-liquid injection factor decreased with increasing the liquid velocity at position 1 and 3. The shear stress increases with the increasing of gas-liquid injection factor and the liquid velocity improves with the increasing of gas-liquid injection factor. The middle location between the entrance and the rear points of air input showed efficient liquid velocity which might be due to the profitable rectilinear and lower fiber packing density.

The relationship between the local fouling along the fiber position and liquid velocity are important. Irreversible fouling resistance (R_{ir}) of the fiber position is significant in a local region of high suction pressure near the suction point of the fiber (position 1). The ratio of R_{ir}/R_m and R_{ir}/R_r of position 1 was highest compared to the position 2 and 3. Irreversible fouling resistances results confirmed the preferential deposition of foulants near the suction part of the fiber where the local suction pressure is the highest and correspondingly, more particles are accumulated to the membrane surface.

Reference

1. C. Cabassud, S. Laborie, and J. M. Laine, “How to slug flow can improve ultrafiltration flux in organic hollow fibers”, *J. Membr. Sci*., **128**, 93 (1997).
2. M. Bonin, C. Lagane, and C. Fonade, “Influence of a gas/liquid teo-phase flow on the ultrafiltration and microfiltration performances: case of a ceramic flat sheet membrane”, *J. Membr. Sci.*, **180**, 93 (2000).
3. M. Mercier, C. Fonade, and C. Lafforgue-Delorme, “How to slug flow can enhance the ultrafiltration flix in mineral tubular membranes”, *J. Membr. Sci.*, **128**, 103 (1997).
4. O. S. Kwon, H. S. Yoon, Y. K. Choi, and S. H. Noh, “Variation of superficial velocity of a submerged module (YEF) by module size and aerator type”, *Desalination*, **233**, 319 (2008).
5. T. Ueda, K. Hata, Y. Kikuoka, and O. Seino, “Effect of aeration on suction pressure in a submerged membrane bioreactor”, *Wat. Res*., **31**, 489 (1997).
6. R. Liu, C. Wang, L. Chen, and Y. Qian, “Study on hydrauric characteristics in a submerged membrane bioreactor process”, *Process Biochemistry*, **36**, 249 (2000).
7. L. Vera, R. Villarroel, S. Delgado, and S. Elmaleh, “Enhancing microfiltration through an inorganic tubulrar membrane by gas sparging”, *J. Membr. Sci*., **165**, 47 (2000).
8. A. Sofia, W. J. Ng, and S. L. Ong, “Enhancing design approaches for minimum fouling in submerged MBR”, *Desalination*, **160**, 67 (2004).
9. H. Prieske, A. Drews, and M. Kraume, “Prediction of the circulation velocity in a membrane bioreactor”, *Desalination*, **231**, 219 (2008).
10. I. H. Won, D. C. Kim, and K. Y. Chung, “Transmembrane Pressure of the Sinusoidal Flux Continuous Operation Mode for the Submerged Flat-sheet Membrane Bioreator in Coagulation Dosage”, *Membr. J*., **25**, 7 (2015).
11. J. H. Kim and F. A. DiGiano, “Defining critical flux in submerged membrane: Influence of length-distributed flux”, *J. Membr. Sci.*, **280**, 752 (2006).
12. S. Chang and A. G. Fane, “The effect of fiber diameter on filtration and flux distribution-relevence to submerged hollow fiber modules”, *J. Membr. Sci*., **184**, 221 (2001).
13. Z. F. Cui, S. Chang, and A. G. Fane, “The use of gas bubbling to enhance membrane process”, *J. Membr. Sci*., **221**, 1 (2003).
14. Y. K. Choi, C. S. Kim, M. S. Cho, O. S. Kwon, S. H. Noh, H. W. Hur, S. K. Park, K. H.Yeon, S. D. Yoon, and I. H. Yeo, “Effect of the aeration

rate on the water velocity distribution in submerged hollow fiber modules", Proceedings of AMS5 Conference, Kobe, Japan (2009).
15. C. Cabassud, S. Laborie, L. Durand-Bourlier, and J. M. Lainė, "Air sparging in ultrafiltration hollow fibers: relationship between flux enhancement, cake characteristics any hydrodynamic parameters", *J. Membr. Sci*., **181**, 57 (2001).
16. D. Pfleger, S. Gomes, N. Gibert, and H.-G. Wagner, "Hydrodynamic simulations of laboratory scale bubble columns fundamental studies of Eulerian-Eulerian modeling approach", *Chem. Eng. Sci.*, **54**, 5091 (1999).
17. P. Spicka, M. M. Dias, and J. C. B. Lopes, "Gas-liquid flow in a 2D column: Comparison between experimental data and CFD modeling", *Chem. Eng. Sci.*, **56**, 6367 (2001).
18. E. N. C. Duc, L. Fournier, C. Levecq, B. Lesjean, P. Grelier, and A. Tazi-Pain, "Local hydrodynamic investigation of the aeration in a submerged hollow fibre membrane cassette", *J. Membr. Sci.*, **312**, 264 (2008).
19. M. Simmonet, C. Gentric, E. Olmos, and N. Midoux, "Experimental determination of the drag coefficient in a swarm of bubbles", *Chem. Eng. Sci.*, **62**, 858 (2007).
20. J. Lin, M. Han, T. Wang, T. Zhang, J. Wang, and Y. Jin, "Influence of the gas distributor on the local hydrodynamic behavior of an external loop airlift reactor", *Chem. Eng. J.*, **102**, 51 (2004).
21. M. Cheryan, "Ultrafiltration and Microfiltration Handbook", Technomic Publishing (1998).
22. M. Mercier, C. Fonade, and C. Lafforgue-Delorme, "Influence of flow regime on the efficiency of a gas-liquid two-phase medium filtration", *Biotech. Techniques*, **9**, 853 (1995).
23. N. V. Ndinisa, D. E. Wiley, and D. F. Fletcher, "Computational fluid dynamics simulations of taylor bubbles in tubular membrane-Model validation and application to laminar flow system", *Chem. Eng. Res. & Design*, **83**, 40 (2005).
24. N. V. Ndinisa, A. G. Fane, D. E. Wiley, and D. F. Fletcher, "Fouling control in a submerged flat membrane system: Part II-Two-phase flow characterization and CFD simulations", *Sep. Sci. Tech.*, **41**, 1411 (2006).
25. J. H. Kim and F. A. DiGiano, "Particle fouling in submerged microfiltration membranes: effects of hollow-fiber length and aeration rate", *AQUA*, **55**, 535 (2006).
26. I. S. Chang, P. Le Clech, B. Jefferson, and S. Jude, "Membrane fouling in membrane bioreactors for wastewater treatment", *J. Environ. Eng.*, **128**, 1018 (2002).